



# Ion exchange resins as catalysts for the liquid-phase dehydration of 1-butanol to di-n-butyl ether



M.A. Pérez, R. Bringué, M. Iborra, J. Tejero\*, F. Cunill

Department of Chemical Engineering, University of Barcelona, C/Martí i Franquès, 1, 08028 Barcelona, Spain

## ARTICLE INFO

### Article history:

Received 13 January 2014

Received in revised form 14 May 2014

Accepted 15 May 2014

Available online 24 May 2014

### Keywords:

Di-n-butyl ether (DNBE)

Ion-exchange resins

1-Butanol dehydration

## ABSTRACT

This work reports the production of di-n-butyl ether (DNBE) by means of 1-butanol dehydration in the liquid phase on acidic ion-exchange resins. Dehydration experiments were performed at 150 °C and 40 bar on 13 styrene-codivinylbenzene ion exchangers of different morphology. By comparing 1-butanol conversions to DNBE and initial reaction rates it is concluded that oversulfonated resins are the most active catalysts for 1-butanol dehydration reaction whereas gel-type resins that swell significantly in the reaction medium as well as the macroreticular thermostable resin Amberlyst 70 are the most selective to DNBE. The highest DNBE yield was achieved on Amberlyst 36. The influence of typical 1-butanol impurities on the dehydration reaction were also investigated showing that the presence of 2-methyl-1-propanol (isobutanol) enhances the formation of branched ethers such as 1-(1-methylpropoxy) butane and 1-(2-methylpropoxy) butane, whereas the presence of ethanol and acetone yields ethyl butyl ether and, to a much lesser extent, diethyl ether.

© 2014 Elsevier B.V. All rights reserved.

## 1. Introduction

Dependence on fossil fuels has raised two main concerns: on one hand, the associated environmental effects; on the other, oil reserves limitation and future depletion. Given the severity of these threats the European Union has ruled increasingly stringent specifications for: (1) quality of petrol, diesel and gas-oil (Directive 2009/30/EC); (2) emissions from light passenger and commercial vehicles (Regulation EC 715/2007); and (3) promotion of the use of energy from renewable sources, setting a mandatory 10% minimum target to be achieved by all Member States for the share of biofuels in transport petrol and diesel consumption by 2020 (Directive 2009/28/EC).

Although very efficient, diesel engines have had difficulties achieving desirable emission targets, especially for soot and NO<sub>x</sub> formation [1]. Reformulation of diesel fuel to include oxygenates has proven to be an effective way to provide satisfactory engine power and cleaner exhaust without modification of existing diesel engines [2–5].

A number of oxygenates have been considered as components for diesel fuel including various alcohols, ethers and esters. Alcohols have several drawbacks: high water solubility, which can cause phase separation problems; high Reid vapor pressure (RVP), which

may lead to the plugging of the fuel flow by increasing the vapor pressure; high volatility, which increases the volatile organic compounds emissions; high latent heat of vaporization, which raises cold start-up and drivability issues; and low heating value [6]. Vegetable oil methyl esters have a number of properties non suitable for diesel fuels such as higher boiling point, viscosity, and surface tension that may contribute to increase the NO<sub>x</sub> emissions [7]. On the other hand, ethers show the best properties for diesel blends such as high cetane number, cold flow properties and mixture stability. In a comprehensive study on the blending properties of different oxygenates in diesel fuel, including monoethers, polyethers and esters, it was observed that linear monoethers with more than 9 carbon atoms showed the best balance among blending cetane number and cold flow properties which are measured by the Cloud Point (CP) and the Cold Filter Plugging Point (CFPP) [8]. Linear ethers have also shown to be effective in reducing diesel exhausts such as CO, particulate matter and unburned hydrocarbons and to substantially improve the trade-off between particulate and NO<sub>x</sub> due to the presence of oxygen in the ether molecules [9].

It is quoted in the open literature that linear symmetrical ethers are produced by bimolecular dehydration of primary alcohols over acid catalysts [10,11]. Nowadays the main synthesis route of primary alcohols is based on the oxo process. It consists of selective hydroformylation and hydrogenation of linear olefins from fluid catalytic cracking in the presence of Rh and Co phosphines [12]. In this way 1-butanol is mainly produced by the oxo synthesis process of propylene in which aldehydes from propylene

\* Corresponding author. Tel.: +34 93 402 1308; fax: +34 93 402 1291.

E-mail addresses: [jtejero@ub.edu](mailto:jtejero@ub.edu), [tejero@angel.qui.ub.es](mailto:tejero@angel.qui.ub.es) (J. Tejero).

## Nomenclature

AAS	amorphous aluminosilicate
ABE	acetone-butanol-ethanol
BET	Brunauer–Emmet–Teller
CFPP	cold filter plugging point
CP	cloud point
$d_{\text{pore}}$	mean pore diameter (nm)
EBE	ethyl butyl ether
DEE	di-ethyl ether
ISEC	inverse steric exclusion chromatography
DNBE	di-n-butyl ether
MSO	mesityl oxide
$n_{\text{DNBE}}$	mole number of di-n-butyl ether (mol)
RVP	Reid vapor pressure
$r_{\text{DNBE}}^0$	initial reaction rate (mol/(h kg of dry catalyst))
$S_j$	selectivity to product $j$
$S_{\text{area}}$	surface area determined from ISEC data ( $\text{m}^2/\text{g}$ )
$S_{\text{BET}}$	BET surface area ( $\text{m}^2/\text{g}$ )
$S/\text{DVB}$	styrene-divinylbenzene
$t$	time (h)
$V_{\text{pore}}$	pore volume ( $\text{cm}^3/\text{g}$ )
$V_{\text{sp}}$	volume of the swollen polymer ( $\text{cm}^3/\text{g}$ )
$W_{\text{cat.}}$	catalyst mass (dried)(g)
WHSV	weight hourly space velocity ( $\text{h}^{-1}$ )
$X_{\text{BuOH}}$	conversion of 1-butanol
$Y_{\text{DNBE}}$	yield of di-n-butyl ether

### Subscripts

BuOBu'	1-(1-methylpropoxy) butane
BuOH	1-butanol
2-BuOH	2-butanol

### Greek letters

$\theta$	porosity (%)
$\rho_s$	skeletal density ( $\text{g}/\text{cm}^3$ )

hydroformylation are hydrogenated to yield 1-butanol. With this hydrogenation step 1-butanol is obtained jointly with 2-methyl-1-propanol (isobutanol) as byproduct. Afterwards, the bimolecular dehydration reaction of the primary alcohol gives the corresponding ether. Although superior alcohols can also be produced from biomass by condensation of bioethanol and/or biomethanol (Guerbet Catalysis) [13], this is still a developing technology which is not yet commercialized [14]. However, biomass fermentation by microorganisms of the genus Clostridium giving place to 1-butanol along with acetone and ethanol (Acetone Butanol Ethanol or ABE fermentation) is being performed on the industrial scale [15,16]. Thus, di-n-butyl ether can be considered a promising oxygenate to blend with diesel fuel as it keeps a good balance between cetane number and cold flow properties [17] and, in addition, it can be obtained from biomass and therefore, it could compete in the biofuel target.

Both an intermolecular dehydration (ether formation) and an intramolecular dehydration (olefin formation) may occur in the alcohol dehydration reaction. The prevailing pathway depends on the reaction conditions as well as the reactant and catalyst used. Solid acids such as zeolites [18], aluminum phosphates [19], amorphous aluminosilicates (AAS) [18], microporous niobium silicates [20],  $\eta$ -alumina [17], and heteropolyacids [21,22] have been tested as catalysts in the dehydration of 1-butanol. In the gas phase selectivity is highly dependent on conversion. Over AlPO<sub>4</sub> the dehydration of 1-butanol gives place mainly to butenes at 1-butanol conversions >75% (fixed-bed reactor, atmospheric

pressure,  $T=300^\circ\text{C}$ ), which suggests that the intramolecular dehydration of 1-butanol to 1-butene and the subsequent isomerization to trans-2-butene and cis-2-butene take place [19]. Butene was the major product for the dehydration reaction on AAS over the whole temperature tested (flow microreactor, 105–185 °C, 1 atm) [18]. At the same set-up and experimental conditions, selectivity to ether over H-ZSM-5 was higher than on AAS at about 2% alcohol conversion, but it decreased remarkably on increasing 1-butanol conversion [18]. In the dehydration of C<sub>5</sub>–C<sub>12</sub> linear alcohols over  $\eta$ -alumina (fixed bed reactor, 250–350 °C, 0–4 MPa, WHSV = 1–4 h<sup>-1</sup>) it was observed that temperatures as high as 300 °C were necessary to achieve over 60% conversion of 1-butanol; selectivity to ethers being lower than 30% [17]. Finally, 1-butanol dehydrated selectively to butenes over microporous niobium silicate as well (150–300 °C, 1 atm) [20]. On the contrary, the liquid phase etherification of 1-butanol to di-n-butyl ether has been studied on heteropolyacids with different heteroatoms (200 °C, 30 bars) showing that 1-butanol dehydrates selectively to di-n-butyl ether achieving over 80% ether selectivity with 1-butanol conversions ranging from 30 to 80% [22].

It is a well-known fact that acidic ion-exchange resins are highly selective catalysts to produce linear symmetrical ethers from n-alcohols, avoiding byproducts as olefins [23–26]. However, to the best of our knowledge the synthesis of di-n-butyl ether has not been reported on ion-exchangers. Thus, the aim of the present paper is to study the liquid-phase dehydration of 1-butanol to DNBE over ion-exchange resins of different morphology and discuss the relationship between resins properties and their catalytic behavior. Influence of typical 1-butanol impurities on 1-butanol dehydration reaction is also discussed.

## 2. Experimental

### 2.1. Chemicals

1-butanol ( $\geq 99.4\%$  pure;  $\leq 0.1\%$  butyl ether;  $\leq 0.1\%$  water) and 2-methyl-1-propanol ( $\geq 99.45\%$  pure;  $\leq 0.05\%$  water) supplied by Acros Organics, acetone ( $\geq 99.8\%$  pure;  $\leq 0.2\%$  water) supplied by Fisher Chemical and ethanol ( $\geq 99.8\%$  pure;  $\leq 0.02\%$  water;  $\leq 0.02\%$  methanol;  $\leq 0.02\%$  2-Butanol) supplied by Panreac were used as reactants.

DNBE ( $\geq 99.0\%$  pure;  $\leq 0.05\%$  water) supplied by Acros Organics, 1-butene ( $\geq 99.0\%$  pure) supplied by Sigma-Aldrich, cis-2-butene ( $\geq 98.0\%$  pure) supplied by TCI and bidistilled water were used for analysis purposes.

### 2.2. Catalysts

Tested catalysts were acidic styrene-codivinylbenzene ion exchange resins: the monosulfonated macroreticular ones Amberlyst 15, Amberlyst 16 and Amberlyst 39 (high, medium and low crosslinking degree, respectively); the oversulfonated macroreticular resins (in which the concentration of  $-\text{HSO}_3$  groups has been increased beyond the usual limit of one group per benzene ring [27]) Amberlyst 35 (high crosslinking degree) and Amberlyst 36 (medium crosslinking degree) which are oversulfonated versions of Amberlyst 15 and Amberlyst 16 respectively; the chlorinated macroreticular resins Amberlyst 70 and CT482; the macroreticular resin sulfonated exclusively at the polymer surface Amberlyst 46; and the monosulfonated gel-type resins Dowex 50W×8, Dowex 50W×4, Amberlyst 31, Dowex 50W×2 and Amberlyst 121 containing from 8 to 2 DVB%. Short names and properties are given in Table 1.

It is well known that ion-exchange resins swell in polar media. As a result, morphology changes and non-permanent pores appear.

**Table 1**  
Properties of tested catalysts.

Catalyst	Short name	Structure <sup>a</sup>	DVB%	Sulfonation type <sup>b</sup>	Acidity <sup>c</sup> (meq H <sup>+</sup> /g)	T <sub>max</sub> <sup>d</sup> (°C)
Amberlyst 15	A-15	M	20	M	4.81	120
Amberlyst 35	A-35	M	20	O	5.32	150
Amberlyst 16	A-16	M	12	M	4.8	130
Amberlyst 36	A-36	M	12	O	5.4	150
CT482	CT-482	M	Medium	M	4.25	190
Amberlyst 70	A-70	M	8	M	2.65	190
Amberlyst 39	A-39	M	8	M	5.0	130
Dowex 50W×8	DOW-8	G	8	M	4.83	150
Amberlyst 31	A-31	G	4	M	4.8	130
Dowex 50W×4	DOW-4	G	4	M	4.95	150
Amberlyst 121	A-121	G	2	M	4.8	130
Dowex 50W×2	DOW-2	G	2	M	4.83	150
Amberlyst 46	A-46	M	High	S	0.87	120

<sup>a</sup> Macroreticular structure (M) or gel-type structure (G).

<sup>b</sup> Monosulfonated (M), oversulfonated (O) or sulfonated only at the polymer surface (S).

<sup>c</sup> Titration against standard base following the procedure described by Fisher and Kunin [28].

<sup>d</sup> Information supplied by manufacturer.

**Table 2** shows the morphological parameters both in dry state and swollen in water of tested resins. As seen, macroreticular resins present BET surface areas ranging between 0.02 and 57.4 m<sup>2</sup>/g (pore volume between 0.0 and 0.328 cm<sup>3</sup>/g). Nevertheless, the same resins show a surface area (and pore volume) increase up to 147–214 m<sup>2</sup>/g (0.333–1.05 cm<sup>3</sup>/g) when swelling in water making clear that new pores with lower pore diameter appear. A useful description of the nature and characteristics of these spaces can be obtained from Inverse Steric Exclusion Chromatography (ISEC) data. In macroreticular resins a part of these new open spaces in the range of mesopores can be characterized by the cylindrical pore model ("true pores"). However, this model is not applicable to describe spaces between polymer chains in the swollen polymer (micropores). A good view of the three-dimensional network of swollen polymer is given by the geometrical model developed by Ogston [29] in which micropores are described by spaces between randomly oriented rigid rods. The characteristic parameter of this model is the specific volume of the swollen polymer (volume of the free space plus that occupied by the skeleton), V<sub>sp</sub>. The Ogston model also allows distinction to be made between zones of swollen gel phase of different density or polymer chain concentration (total rod length per volume unit of swollen polymer, nm<sup>-2</sup>). According

to the Ogston model, the density of polymer chains is described as the total rod length per unit of volume. Fig. 1 shows the distribution of different polymer density zones of swollen catalysts in aqueous phase. As seen, gel-type resins Amberlyst 121, Dowex 50W×2, Amberlyst 31 and Dowex 50W×4 and macroreticular resins with low crosslinking degree Amberlyst 70 and Amberlyst 39 show low polymer densities (0.2–0.8 nm<sup>-2</sup>) typical of an expanded polymer whereas macroreticular resins with medium and high crosslinking degree CT482, Amberlyst 36, Amberlyst 16, Amberlyst 35, Amberlyst 15 and Amberlyst 46 present high chain concentration (1.5–2 nm<sup>-2</sup>) characteristic of a very dense polymer mass. It is to be noted that Dowex50W×8, in spite of being a gel-type resin, shows zones with high polymer density (2 nm<sup>-2</sup>). That behavior is probably due to its high DVB%.

### 2.3. Apparatus

Experiments were carried out in a 100-mL-cylindrical high pressure autoclave made of 316 stainless steel (maximum temperature: 232 °C; pressure range: 0–150 bar). It was equipped with a magnetic drive stirrer and with a 400 W electrical furnace for heating. Temperature was measured by a thermocouple located inside the

**Table 2**  
Morphology of tested catalysts in the dry state and swollen in water.

Catalyst	$\rho_s$ <sup>a</sup> (g/cm <sup>3</sup> )	Dry state			Swollen in water (ISEC method)				
		$S_{BET}$ <sup>b</sup> (m <sup>2</sup> /g)	$V_{pore}$ <sup>c</sup> (cm <sup>3</sup> /g)	$d_{pore}$ <sup>d</sup> (nm)	"True Pores"		Gel polymer		
					$S_{ISEC}$ <sup>e</sup> (m <sup>2</sup> /g)	$V_{ISEC}$ <sup>f</sup> (cm <sup>3</sup> /g)	$d_{pore}$ <sup>d</sup> (nm)	$V_{sp}$ (cm <sup>3</sup> /g)	$\theta_{Total}$ <sup>g</sup> (%)
A-15	1.416	42.01	0.328	31.8	157	0.632	16.1	0.823	51.5
A-35	1.542	28.90	0.210	23.6	166	0.623	15.0	0.736	52.3
A-16	1.401	1.69	0.013	29.7	149	0.384	10.3	1.245	56.2
A-36	1.567	21.00	0.143	27.0	147	0.333	9.1	0.999	52.1
CT-482	1.538	8.7	0.06	26.8	214	1.051	18.5	1.081	69.5
A-70	1.520	0.02			176	0.355	8.1	1.15	56.3
A-39	1.417	0.09	$2.9 \times 10^{-4}$	17.6	181	0.36	7.9	1.451	61.0
DOW8	1.430	0.23						1.627	57.0
A-31	1.426	0.10	$3.3 \times 10^{-4}$	15.3				1.933	63.7
DOW4	1.426	0.01						1.92	63.5
A-121	1.428	0.02	$3.5 \times 10^{-4}$	32.9				3.263	78.5
DOW2	1.426	1.32						2.655	73.6
A-46	1.137	57.4	0.263	19.2	186	0.48	10.3	0.16	0.0

<sup>a</sup> Skeletal density measured by Helium displacement.

<sup>b</sup> BET (Brunauer–Emmett–Teller) surface area.

<sup>c</sup> Pore volume determined by adsorption-desorption of N<sub>2</sub> at 77 K.

<sup>d</sup> Mean pore diameter. Assuming pore cylindrical model:  $4V_{pore}/S_{BET}$  or  $4V_{ISEC}/S_{ISEC}$ .

<sup>e</sup> Surface area determined from ISEC data.

<sup>f</sup> Pore volume determined from ISEC data.

<sup>g</sup> Porosity estimated as  $100(V_{ISEC} + V_{sp} - (1/\rho_s))/(V_{ISEC} + V_{sp})$  in swollen state.

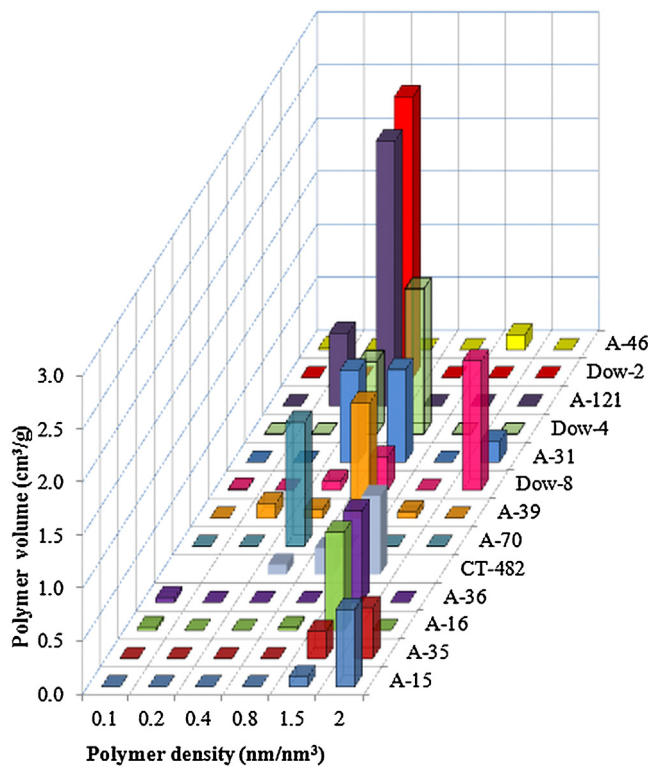


Fig. 1. ISEC pattern in water for used resins.

reactor and stirring speed was measured by a tachometer. Both operation variables were controlled to  $\pm 1^\circ\text{C}$  and  $\pm 1\text{ rpm}$  respectively by an electronic control unit. An injection system attached to the reactor was used to load the catalyst once the operating conditions were reached. One of the outlets of the reactor was connected directly to a liquid sampling valve, which injected  $0.2\text{ }\mu\text{L}$  of pressurized liquid into a gas–liquid chromatograph.

#### 2.4. Analysis

In order to follow the course of the reaction, the composition of the liquid mixture was analyzed on-line by a 7820A GC System equipped with a TCD detector able to measure the presence of water. The capillary column used was a dimethylpolysiloxane HP-Pona ( $50\text{ m}\times 0.200\text{ mm}\times 0.50\text{ }\mu\text{m}$ ). Helium was used as the carrier gas ( $70\text{ mL min}^{-1}$ , constant flow). Chromatograph parameters were: volume injection  $0.2\text{ }\mu\text{L}$ ; split ratio 100:1; injector temperature  $150^\circ\text{C}$ ; oven program:  $45^\circ\text{C}$  for  $5.5\text{ min}$ ,  $50^\circ\text{C min}^{-1}$  up to  $180^\circ\text{C}$  which was held for  $5\text{ min}$ . TCD parameters were: detector temperature  $250^\circ\text{C}$ ; reference flow  $20\text{ mL min}^{-1}$ ; makeup flow  $4.9\text{ mL min}^{-1}$ .

A second GC equipped with a MS (Agilent GC/MS 5973) and chemical database software was used to identify all the species.

#### 2.5. Methodology and calculations

##### 2.5.1. Resin screening

Wet resins (as provided by the supplier) were dried at room temperature for  $24\text{ h}$  prior to mechanical sieving. Resin samples with bead size between  $0.40$  and  $0.63\text{ mm}$  were dried at  $110^\circ\text{C}$ , firstly at  $1\text{ bar}$  for  $2\text{ h}$  and then at  $10\text{ mbar}$  for  $15\text{ h}$ . 1-butanol was charged in the reactor and heated to  $150^\circ\text{C}$ . The reaction mixture was pressurized to  $40\text{ bar}$  by means of  $\text{N}_2$  in order to assure the liquid phase reaction medium. The stirring speed was set at  $500\text{ rpm}$ . After reaching the working temperature,  $1\text{ g}$  of dry catalyst was

injected by means of pneumatic transport. That moment was considered the starting point of reaction. To follow the variation of concentration of reactants and products with time, liquid samples were taken out hourly and analyzed on-line as mentioned above. Total length of the experiments was  $7\text{ h}$ . In all the experiments mass balance was accomplished within  $\pm 8\%$ .

An additional series of experiments was performed over Amberlyst 31 and Amberlyst 15 to test their thermal stability and reusability. These resins have one of the lower maximum operation temperatures within the gel-type group and the macroreticular group respectively (Table 1). Each resin was used for three cycles. In the first cycle fresh catalysts were used following the experimental procedure above mentioned. After a  $7\text{ h}$  experiment the reactor was cooled at the room temperature, catalyst was filtered out from the reaction medium, washed with  $25\text{ mL}$  of methanol, dried at ambient temperature for  $24\text{ h}$  then dried at  $110^\circ\text{C}$ , firstly at  $1\text{ bar}$  for  $2\text{ h}$  and then at  $10\text{ mbar}$  for  $15\text{ h}$  before being subjected to a new reaction cycle.

In each experiment, 1-butanol conversion ( $X_{\text{BuOH}}$ ), selectivity to products ( $S_j$ , the subscript  $j$  corresponding to each formed product) and DNBE yield ( $Y_{\text{DNBE}}$ ) were estimated as follows:

$$X_{\text{BuOH}} = \frac{\text{Moles of 1-butanol reacted}}{\text{Initial moles of 1-butanol}} \quad (1)$$

$$S_{\text{DNBE}} = \frac{\text{Moles of 1-butanol reacted to form DNBE}}{\text{Moles of 1-butanol reacted}} \quad (2)$$

Selectivity to olefins ( $S_{1\text{-butene}}$ ,  $S_{(E)2\text{-butene}}$  and  $S_{(Z)2\text{-butene}}$ ) branched ether 1-(1-methylpropoxy) butane ( $S_{\text{BuOBu}'}$ ) and 2-butanol ( $S_{2\text{-BuOH}}$ ) were defined similarly.

$$Y_{\text{DNBE}} = \frac{\text{Moles of 1-butanol reacted to form DNBE}}{\text{Initial moles of 1-butanol}} = X_{\text{BuOH}} \cdot S_{\text{DNBE}} \quad (3)$$

In addition, initial reaction rate of DNBE formation ( $r_{\text{DNBE}}^0$ ) was computed from the function of the experimental curve of DNBE mole ( $n_{\text{DNBE}}$ ) vs. time according to:

$$r_{\text{DNBE}}^0 = \frac{1}{W_{\text{cat}}} \left( \frac{dn_{\text{DNBE}}}{dt} \right)_{t=0} \quad (4)$$

Initial turnover frequency for DNBE formation ( $\text{TOF}_{\text{DNBE}}^0$ ) was estimated by dividing  $r_{\text{DNBE}}^0$  by the acid capacity:

$$\text{TOF}_{\text{DNBE}}^0 = \frac{r_{\text{DNBE}}^0}{\text{Acid capacity}} \quad (5)$$

##### 2.5.2. Presence of byproducts in the feed composition

The influence of typical 1-butanol impurities on the dehydration of 1-butanol to DNBE was studied. If 1-butanol is produced by the oxo process the main impurity is isobutanol whereas if it is produced by the ABE fermentation process the impurities are ethanol and acetone. Experiments were carried out with different mixtures of 1-butanol: isobutanol (95:5 and 90:10 wt%) and 1-butanol: ethanol:acetone (95:2.5:2.5 and 90:5:5 wt%) over the highly selective resins Amberlyst 70, Amberlyst 31 and Amberlyst 121. The experimental procedure and reaction conditions were the same as for catalyst testing:  $1\text{ g}$  of dry catalyst, catalyst bead size between  $0.400$  and  $0.630\text{ mm}$ ,  $150^\circ\text{C}$ ,  $40\text{ bar}$ ,  $500\text{ rpm}$ , and  $7\text{ h}$ .

## 3. Results and discussion

### 3.1. Reaction network

Dehydration of 1-butanol over the ion exchange resins tested leads to the formation of di-n-butyl ether as main product. Detected byproducts were  $C_4$  olefins (1-butene, trans- and cis-2-butene), the branched ether 1-(1-methylpropoxy) butane and, in much

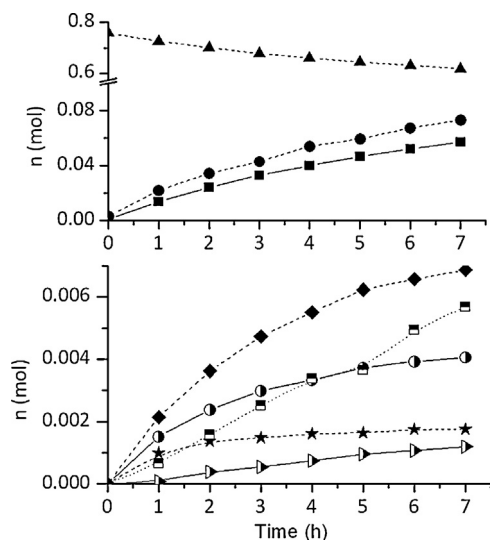


**Fig. 2.** Evolution of reaction medium composition with time (1 g of Amberlyst-15, catalyst bead size = 0.400–0.630 mm,  $T = 150^\circ\text{C}$ ,  $P = 40$  bar, 500 rpm): (▲) 1-butanol; (●) water; (■) DNBE; (★) 1-butene; (◆) trans-2-butene; (○) cis-2-butene; (■) 1-(1-methylpropoxy)butane; (►) 2-butanol.

smaller amount, 2-butanol. Fig. 2 shows the evolution of the liquid phase composition over the course of an experiment conducted on Amberlyst 15. The product distribution on all tested resins is similar although it should be pointed out some significant differences: (1) over macroreticular resins with low crosslinking degree (Amberlyst 39 and Amberlyst 70) and gel type resins (Amberlyst 31, Amberlyst 121, Dowex 50×4 and Dowex 50×2) 2-butanol was not detected; (2) after 7 hours reaction time most resins showed higher selectivity to 2-butenes than to 1-butene except for Amberlyst 70, Amberlyst 121 and Dowex 50×2. This fact may be due to the very low total amount of butenes formed on those resins.

Distribution of products suggests the reaction network shown in Fig. 3. Dehydration of 1-butanol to di-n-butyl ether (DNBE) is the main reaction (R1). Dehydration to olefins is the main side reaction (R2). The fact that at very low olefin concentration the major  $\text{C}_4$  product was 1-butene whereas when the olefin

concentration increases 2-butenes are favored, especially trans-2-butene, indicates that 1-butanol dehydrates to 1-butene which in turn isomerizes to trans-2-butene and cis-2-butene (R3); the trans-isomer being thermodynamically more stable. The resin sites are also active for catalyzing the reverse reactions of (R1) and (R2), ether hydrolysis (R4) and olefin hydration (R5). When olefin hydration takes place, the alcohol that is formed is no longer a primary alcohol. In addition to double bond isomerization, 2-butenes could be formed by hydration of 1-butene to 2-butanol and its subsequent dehydration, giving place to any of the three  $\text{C}_4$  olefins. From the fact that 1-(1-methylpropoxy)butane was detected over all the resins despite the nonexistence of 2-butanol on some catalysts, it is inferred that the branched ether could be preferably formed by 1-butanol reaction with a  $\text{C}_4$  olefin (R6) instead of by the reaction between 1-butanol and 2-butanol. Furthermore, the absence of 2,2'-oxydibutane indicates that intermolecular dehydration of two molecules of 2-butanol is not taking place, probably due to the low concentration of the secondary alcohol in the reaction medium.

### 3.2. 1-Butanol conversion, initial reaction rate, selectivity to DNBE and DNBE yield

Table 3 shows 1-butanol conversion, selectivity to DNBE and byproducts, and yield of DNBE at 7 h reaction time. Initial reaction rate and turnover frequency of DNBE synthesis are also given. The data has a relative experimental error lower than  $\pm 4\%$  for  $X_{\text{BuOH}}$ ,  $\pm 1\%$  for  $S_{\text{DNBE}}$ ,  $\pm 5\%$  for  $Y_{\text{DNBE}}$  and  $\pm 7\%$  for  $r^0_{\text{DNBE}}$  and  $\text{TOF}^0_{\text{DNBE}}$ . Due to the low concentration of byproducts in the reaction medium,  $S_{\text{byproducts}}$  data has in some cases a relative experimental error up to  $\pm 20\%$ .

Taking into account that some preliminary extended duration experiments ( $>72$  h) showed that equilibrium conversions are higher than 85% at the working conditions, it is seen that at the end of the experiments the reaction medium is still far from equilibrium. From data of Table 3 it is seen that the most active resins are the oversulfonated resins Amberlyst 36 and Amberlyst 35, whereas the most selective ones are Amberlyst 121 > Dowex 50W×2 > Amberlyst 70 > Amberlyst 46 > Dowex 50W×4 > Amberlyst 31. Resins Amberlyst 16 > Amberlyst

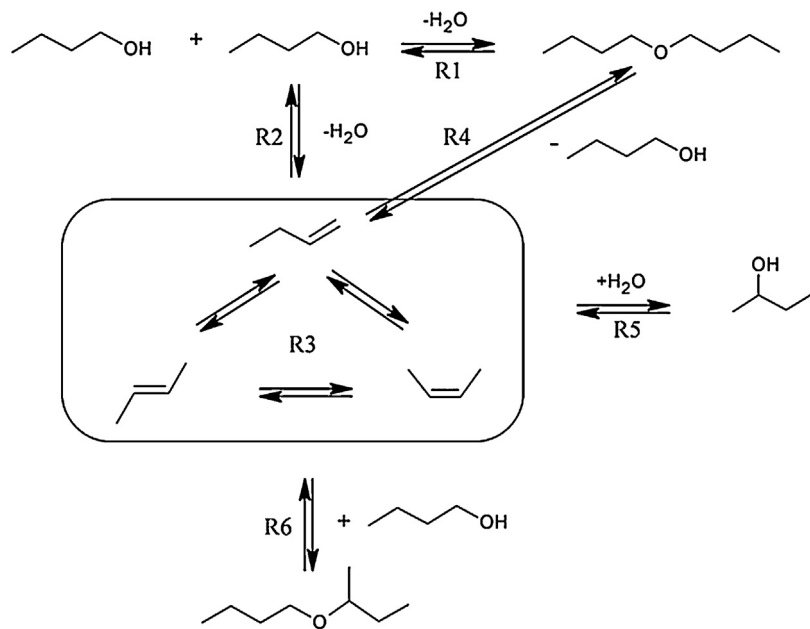


**Fig. 3.** Scheme of reaction network.

**Table 3**

Conversion of 1-butanol, selectivity to DNBE and byproducts, yield to DNBE at 7 h reaction, initial reaction rate and turnover frequency for DNBE formation (1 g catalyst, catalyst bead size = 0.400–0.630 mm,  $T = 150^\circ\text{C}$ ,  $P = 40$  bar).

Catalyst	$X_{\text{BuOH}}$ (%)	$S_{\text{DNBE}}$ (%)	$S_{1\text{-Butene}}$ (%)	$S_{(\text{E})2\text{-Butene}}$ (%)	$S_{(\text{Z})2\text{-Butene}}$ (%)	$S_{2\text{-BuOH}}$ (%)	$S_{\text{BuOBu'}}$ (%)	$Y_{\text{DNBE}}$ (%)	$r^0_{\text{DNBE}}$ (mol/h kg)	$\text{TOF}^0_{\text{DNBE}}$ (mol/h eq $\text{H}^+$ )
A-15	18.4	81.7	1.27	4.89	2.74	0.890	8.56	15.0	15.6	3.25
A-35	22.2	74.8	1.38	6.35	3.46	1.33	12.7	16.6	22.9	4.30
A-16	19.9	92.9	0.753	1.65	0.994	0.343	3.33	18.5	17.2	3.59
A-36	23.2	86.4	0.934	3.30	1.87	0.725	6.76	20.1	28.1	5.20
CT-482	19.3	95.8	0.707	0.917	0.634	0.215	1.74	18.4	15.8	3.72
A-70	14.1	98.7	0.479	0.120	0.096	Trace	0.595	14.0	10.3	3.90
A-39	19.4	97.1	0.613	0.559	0.407	0.0798	1.21	18.8	16.1	3.21
Dow-8	19.4	96.2	0.644	0.795	0.551	0.191	1.60	18.7	15.8	3.26
A-31	18.9	98.1	0.513	0.321	0.235	0.0431	0.759	18.5	14.5	3.02
Dow-4	18.6	98.4	0.481	0.265	0.215	Trace	0.679	18.3	13.8	2.79
A-121	17.6	99.1	0.423	0.0118	Trace	0	0.440	17.5	13.2	2.75
Dow-2	18.4	98.9	0.379	0.151	0.136	0	0.458	18.2	12.7	2.64
A-46	3.25	98.7	Trace	Trace	Trace	0	1.32	3.21	1.64	1.88

36 > Amberlyst 15 > Amberlyst 35 show the lowest selectivity to ether.

By plotting the selectivity to DNBE as a function of  $X_{\text{BuOH}}$  (Fig. 4) it is shown that, for all tested resins,  $S_{\text{DNBE}}$  initially decreases and then stabilizes. As a consequence it can be concluded that at these alcohol conversions, the differences observed in  $S_{\text{DNBE}}$  after 7 h of reaction time are not due to the different reaction extent on each catalyst. On the contrary, they are a consequence of the resins properties, in particular morphology and acid capacity.

Fig. 5 shows the response surfaces for conversion and selectivity as a function of acid capacity and  $V_{\text{sp}}$ , which, together with polymer chain density, is a suitable way of characterizing the polymeric

structure of the resins gel type phase. As seen, acid capacity is the parameter which plays the most important role regarding resins activity as it can be inferred from the almost vertical arrangement of colors in the response surface of Fig. 5(a). Nevertheless, selectivity to DNBE is influenced by both acid capacity and resin structure as it can be drawn from the diagonal arrangement of colors in the response surface of Fig. 5(b).

In order to elucidate the influence of acid capacity and polymer morphology on resins behavior, obtained data have been arranged as shown in Fig. 6. In this way it is easy to compare on one hand, the behavior of resins having the same acid capacity but different polymeric structure and, on the other hand, resins with similar values of swollen polymer volume but different acid capacity. Data corresponding to Amberlyst 46 have been omitted in Fig. 6(a), (c) and (d) for the sake of clarity.

From Fig. 6 it can be assumed that a higher acid capacity is essential for a more active catalyst (Fig. 6 (a) and (c)) but it also seems to affect the catalyst selectivity to DNBE in a negative way (Fig. 6 (b)). Regarding polymer morphology, it plays a decisive role on resin selectivity to DNBE and, although not as significant as acid capacity, it also influences catalytic activity. These facts can be observed by comparing resins with similar acid capacity but different pore structure: (1) Amberlyst 35 and Amberlyst 36 (5.3 meq  $\text{H}^+$ /g), and (2) Amberlyst 15, Amberlyst 16, Amberlyst 39, Dowex 50W×8, Amberlyst 31, Dowex 50W×4, Amberlyst 121 and Dowex 50W×2 (around 4.8 meq  $\text{H}^+$ /g). It can be seen that, as  $V_{\text{sp}}$  rises,  $S_{\text{DNBE}}$  progressively increases until reaching an almost constant value of about 98–99% with gel-type resins containing  $\leq 4\%$  DVB (Fig. 6 (b)). However, in spite of the improvement in catalytic activity observed when the  $V_{\text{sp}}$  increases from  $0.823 \text{ cm}^3/\text{g}$  (Amberlyst 15) to  $1.245 \text{ cm}^3/\text{g}$  (Amberlyst 16) a further increase in  $V_{\text{sp}}$  leads to a slight reduction of the resin activity (Fig. 6(a) and (c)).

It is a well-established fact that the alcohol dehydration reaction occurs mainly in the swollen polymer mass [23]. Dehydration to ether follows an  $S_N2$  reaction mechanism in which 2 alcohol molecules are involved, whereas dehydration to olefins occurs by a monomolecular reaction of elimination, E1 [30]. As Fig. 1 shows, the tested resins have zones of different density or polymer chain concentration in the swollen polymer mass ranging from 0.1 to  $2.0 \text{ nm}/\text{nm}^3$ . Very high polymer concentration ( $2 \text{ nm}/\text{nm}^3$ ) entails a very dense polymer mass, poorly accessible to 1-butanol which leads to a lower catalytic activity. Furthermore, in this dense polymer zone the  $S_N2$  reaction is limited to a great extent by steric hindrance and the occurrence of the E1 reaction increases, hence giving place to lower  $S_{\text{DNBE}}$ . On the other hand, low polymer concentration corresponding to a greatly expanded polymer enhances selectivity to DNBE. However, too low polymer concentration gives place to a significant distance among its active centers. In this

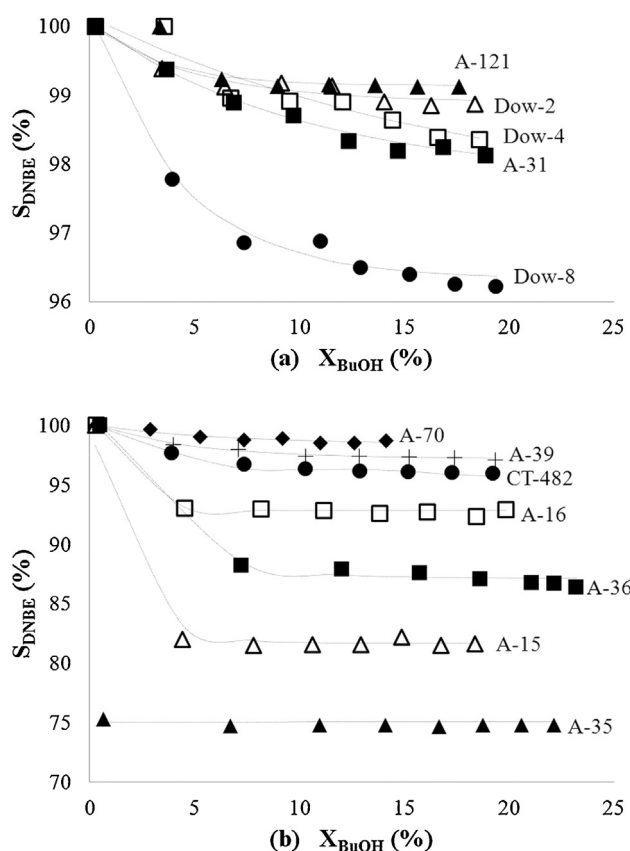
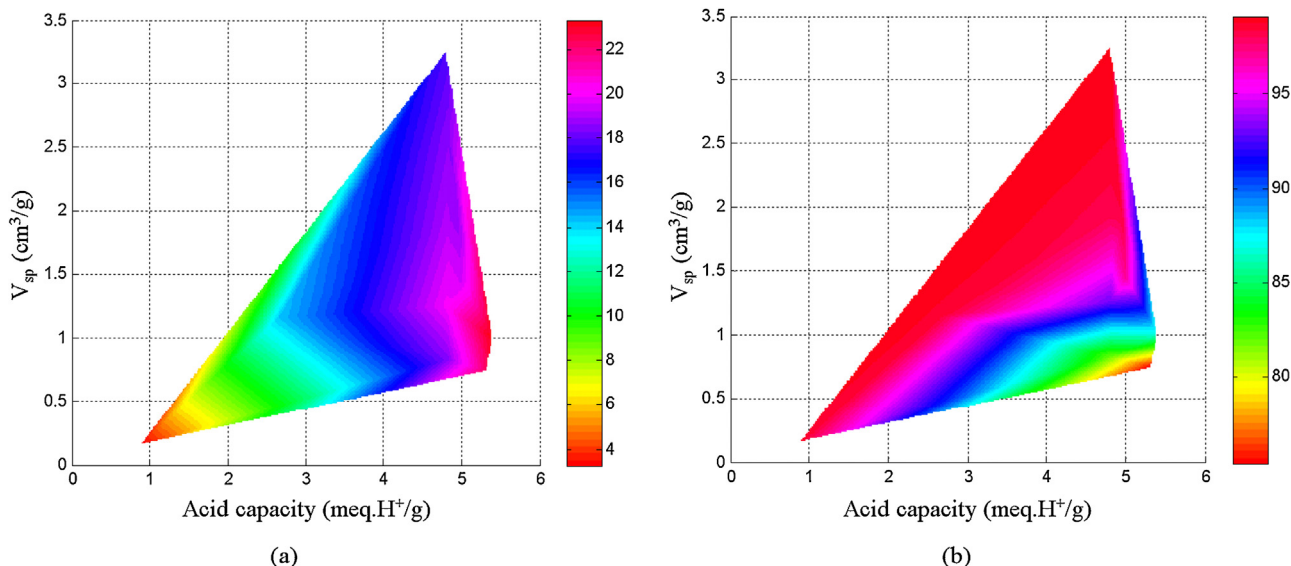
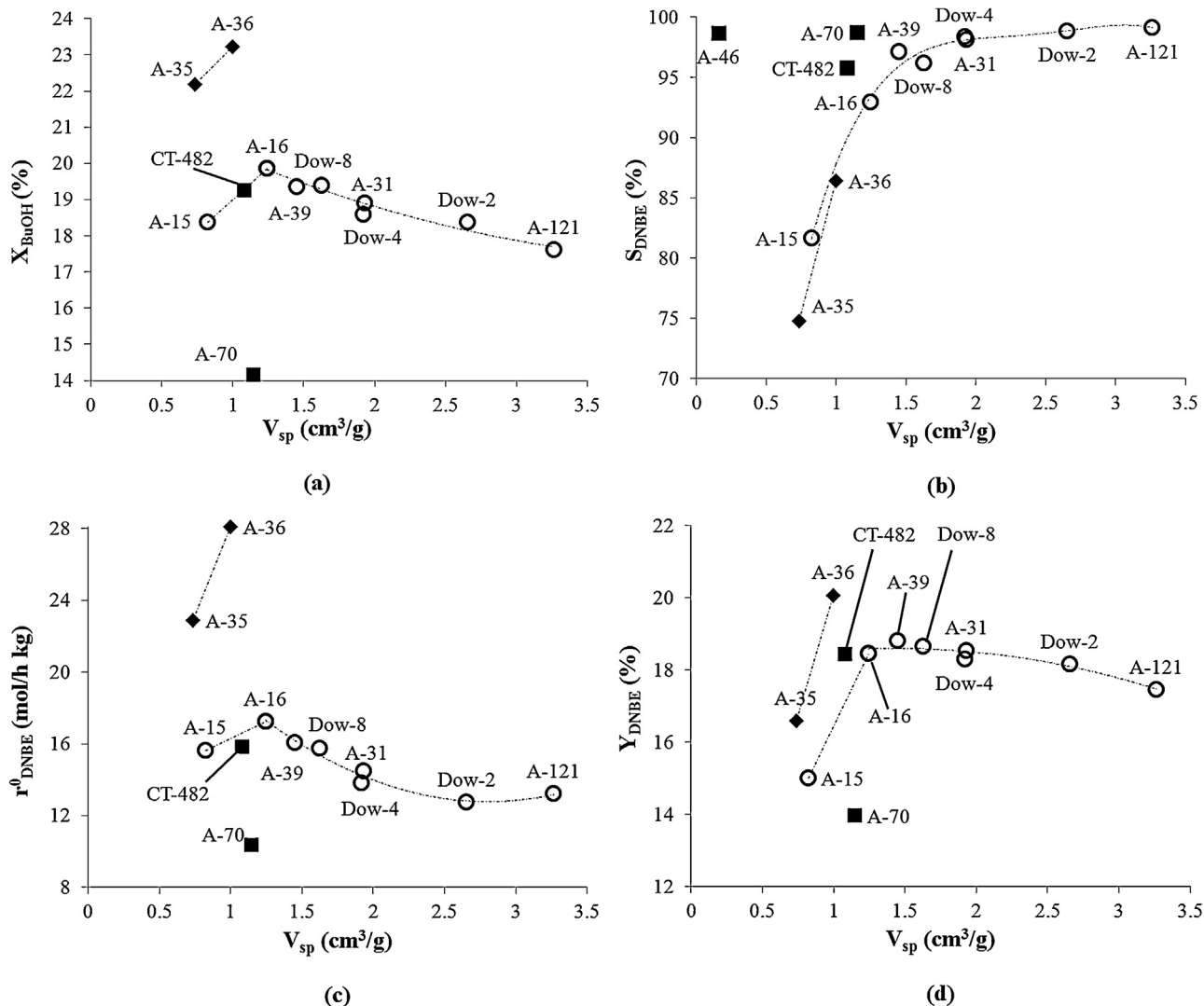


Fig. 4.  $S_{\text{DNBE}}$  as a function of 1-butanol conversion (1 g catalyst, catalyst bead size = 0.400–0.630 mm,  $T = 150^\circ\text{C}$ ,  $P = 40$  bar, 500 rpm): (a) gel-type resins: (▲) A-121, (■) A-31, (△) Dow-2, (□) Dow-4, (●) Dow-8; (b) macroreticular resins: (◆) A-70, (+) A-39, (◇) CT-482, (□) A-16, (△) A-15, (■) A-36, (▲) A-35.



**Fig. 5.** Response surfaces for: (a) 1-butanol conversion; (b) selectivity to DNBE as a function of  $V_{sp}$  and Acid Capacity.  $t = 7 \text{ h}$ , 1 g catalyst, catalyst bead size = 0.400–0.630 mm,  $T = 150^\circ\text{C}$ ,  $P = 40 \text{ bar}$ , 500 rpm.



**Fig. 6.** Influence of  $V_{sp}$  on: (a) 1-BuOH conversion; (b) selectivity to di-n-butyl ether; (c) initial reaction rate for DNBE synthesis; (d) DNBE yield.  $t = 7 \text{ h}$ , 1 g catalyst, catalyst bead size = 0.400–0.630 mm,  $T = 150^\circ\text{C}$ ,  $P = 40 \text{ bar}$ , 500 rpm. (○) resins with 4.8 meq H<sup>+</sup>/g; (◆) resins with 5.3 meq H<sup>+</sup>/g; (■) resins with other values of acid capacity.

case the probability of disposing the precise orientation of sulfonic groups to form the reaction intermediate lessens and resins activity decreases. Thus, medium values of polymer chain concentration may favor 1-butanol conversion. That could explain the behavior observed in Fig. 6(a) and (c) where, among resins with acid capacity around 4.8 meq. H<sup>+</sup>/g, Amberlyst 16 ( $V_{sp} = 1.245 \text{ cm}^3/\text{g}$ ; polymer density = 0.8–1.5 nm/nm<sup>3</sup>) shows a 1-butanol conversion and initial reaction rate higher than those determined on gel-type resins (which have higher  $V_{sp}$  but polymer densities ranging between 0.2 and 0.8 nm/nm<sup>3</sup>). TOPO<sub>DNBE</sub> data (Table 3) confirm that resins with medium  $V_{sp}$  values shows higher reaction rates per catalytic site.

As for thermostable resins Amberlyst 70 and CT482, the latter has a  $V_{sp}$  of 1.081 cm<sup>3</sup>/g (Table 2) and an acid capacity of 4.25 meq. H<sup>+</sup>/g (Table 1). This value of acid capacity is not very different from 4.8 meq. H<sup>+</sup>/g and, as seen in Fig. 6(a) and (c), catalytic activity of resin CT482 is in agreement with data obtained for resins with 4.8 meq. H<sup>+</sup>/g. Amberlyst 70 shows lower 1-butanol conversion because of its low acid capacity (2.65 meq. H<sup>+</sup>/g, Table 2). Furthermore, it can be seen that selectivity to the linear ether over Amberlyst 70, as well as over Amberlyst 46, is equal to the maximum  $S_{DNBE}$  value found which corresponds to the gel-type resins Amberlyst 121 and Dowex 50W×2. This high selectivity (and therefore, high DNBE content in the final product) is extremely desirable from an environmental standpoint, in addition to the obvious impact on capital requirements and operating costs.

As seen in Fig. 6(d) the highest DNBE yield is achieved on Amberlyst 36, nonetheless, gel-type resins and Amberlyst 70 are more selective to the linear ether which makes them more appropriate for industrial use. Among them, Amberlyst 70 can be considered as the most suitable catalyst due to its thermal stability.

Finally, Fig. 7 shows the combined effect of acid capacity and  $V_{sp}$  on  $S_{DNBE}$  for all tested resins. As can be seen,  $S_{DNBE}$  correlates quite well with acid capacity/ $V_{sp}$  ratio showing that selectivity to DNBE increases as the number of acid sites per volume unit of swollen polymer (acid density) decreases.

### 3.3. Thermal stability and reusability tests

Thermal stability and reusability tests were conducted over Amberlyst 15 and Amberlyst 31. These two resins were selected because they have a maximum operating temperature very much lower than 150 °C. Afterwards, BET surface area and acid capacity were measured and compared to those of fresh catalyst. As shown in Table 4 both resins experience some loss of sulfonic acid groups after 3 cycles (fresh resin plus two reused cycles; 21 h of accumulated working time). BET surface area increases moderately in the case of Amberlyst 15. Despite the small morphological and acid

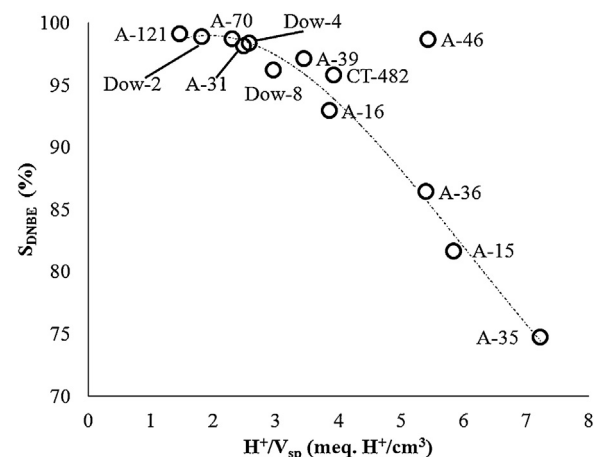


Fig. 7. Selectivity to di-n-butyl ether at  $t = 7\text{ h}$  (1 g catalyst, catalyst bead size = 0.400–0.630 mm,  $T = 150^\circ\text{C}$ ,  $P = 40\text{ bar}$ , 500 rpm) as a function of  $\text{H}^+/\text{V}_{sp}$ .

Table 4

Acid capacity and BET surface area of fresh and reused catalysts after 3 reaction cycles (7 h, 150 °C, 40 bar).

Catalyst	Acid site loss <sup>a</sup> (%)	$S_{BET}^b$ (m <sup>2</sup> /g)	
		Fresh	Reused
Amberlyst 15	11.6 ± 3.3	42.01	43.7
Amberlyst 31	8.6 ± 1.9	0.10	0.10

<sup>a</sup> Titration against standard base following the procedure described by Fisher and Kunin [28].

<sup>b</sup> BET (Brunauer–Emmet–Teller) surface area.

capacity change, the performance of the two resins remains constant throughout the 3 cycles, as it can be seen in Fig. 8, pointing out that results are not influenced by thermal deactivation and resins can be reused a few cycles. In order to take into account the differences in initial alcohol and catalysts mass (due to small catalysts losses in recovering and cleaning the resin operations), the factor  $X_{1-\text{BuOH}} \cdot n^0_{1-\text{BuOH}} / W_{\text{cat}}$  is used instead of  $X_{1-\text{BuOH}}$ . The differences observed for  $r^0_{DNBE}$  between Fig. 8 data and values gathered in Table 2 for Amberlyst 31 and Amberlyst 15 are due to the fact that in this series of experiments the injector was not used. Thus, catalyst was charged into the reactor and then heated to 150 °C; the moment at which this temperature was reached was considered as the beginning of the experiment (zero time). It is to be noted that despite this change of methodology the results are quite similar. It is concluded from these reuse experiments that data reported in

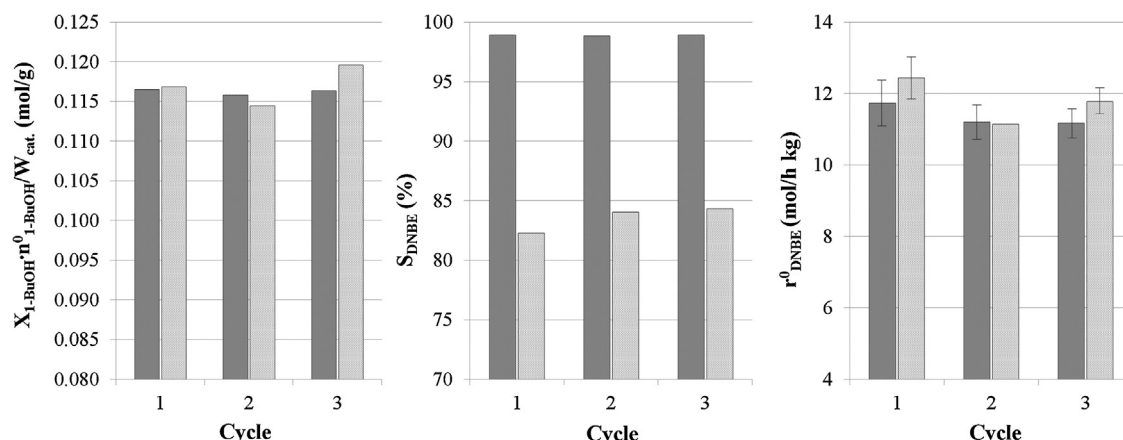
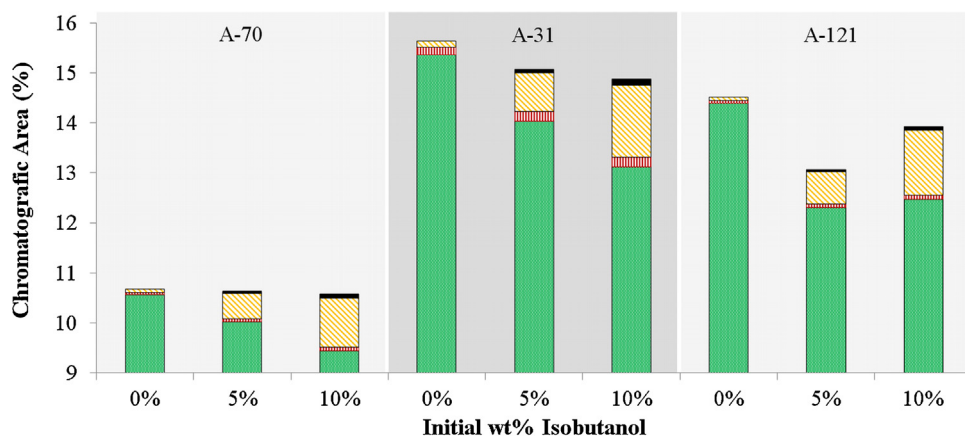
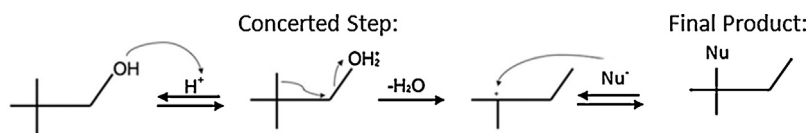


Fig. 8. Conversion of 1-butanol ( $X_{\text{BuOH}} \cdot n^0_{\text{BuOH}} / W_{\text{cata}}$ ) and selectivity to DNBE ( $S_{\text{DNBE}}$ ) at 7 h reaction and initial reaction rate for DNBE formation (1 g catalyst, catalyst bead size = 0.400–0.630 mm,  $T = 150^\circ\text{C}$ ,  $P = 40\text{ bar}$ ). (■) Amberlyst 31; (□) Amberlyst 15.



**Fig. 9.** Influence of 2-methyl propanol on the dehydration of 1-butanol to DNBE at 7 h reaction.  $T = 150^\circ\text{C}$ ,  $P = 40$  bar, 500 rpm, 1 g catalyst, catalyst bead size = 0.400–0.630 mm: (■) DNBE; (▨) Olefins; (▨) 1-(1-methylpropoxy) butane; (■) 1-(2-methylpropoxy) butane.



**Fig. 10.** Mechanism of Concerted Alkyl Shift.

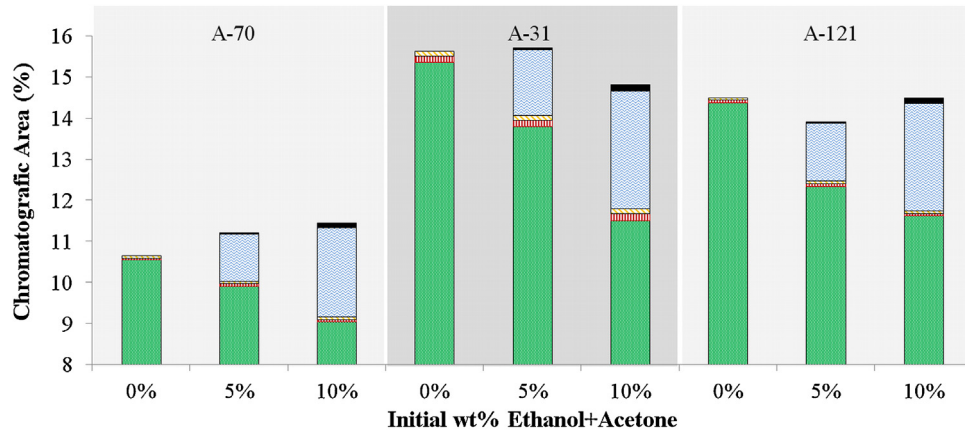


**Fig. 11.** Influence of ethanol and acetone on the dehydration of 1-butanol to DNBE at 7 h reaction.  $T = 150^\circ\text{C}$ ,  $P = 40$  bar, 500 rpm, 1 g catalyst, catalyst bead size = 0.400–0.630 mm: (■) DNBE; (▨) Olefins; (▨) 1-(1-methylpropoxy) butane; (▨) Ethyl butyl ether; (■) Diethyl ether.

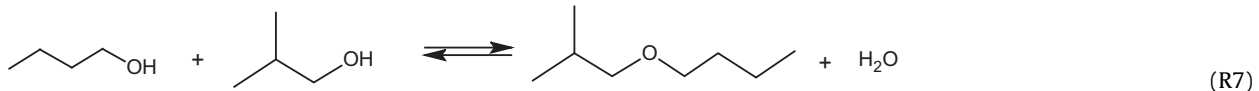
**Table 3** are reliable. It can be accepted that accessible zone of resins increases on losing active centers, and this effects are mutually balanced. However, as resins show a clear trend to morphological instability it is suitable to use resins with high thermal stability such us Amberlyst 70 for industrial application.

#### 3.4. Influence of typical 1-butanol impurities

##### 3.4.1. Influence of 2-methyl-1-propanol (isobutanol)

**Fig. 9** shows the influence of isobutanol presence on the dehydration of 1-butanol to DNBE at 7 h reaction time. As seen, the trend is very similar over the three tested resins: the selectivity to DNBE decreases upon increasing the initial concentration of the branched alcohol mainly due to the increase in 1-(1-methylpropoxy)butane formation. It is quoted in the open literature that alcohols can undergo alkyl group transpositions [31]. In primary alcohols, after

protonation to form the alkyloxonium ion, steric hindrance interferes in the direct displacement of the leaving group (water) by the nucleophile; instead water leaves at the same time as the alkyl group shifts from the adjacent carbon to skip the formation of the unstable primary carbocation. This mechanism is known as "Concerted Alkyl Shift" (**Fig. 10**). Thus, the increasing amounts of 1-(1-methylpropoxy)butane detected when isobutanol is initially present in the reaction medium is explained by the reaction of 1-butanol with the secondary carbocation which results from isobutanol dehydration and alkyl group shift. The rearrangement of products during isobutanol dehydration in the presence of strong Brønsted acid sites is also reported by Kotsarenko and Malysheva [32]. 1-(2methylpropoxy) butane was also detected in the reaction medium over the three tested resins when isobutanol was added into the feed composition. This new branched ether is formed when a molecule of isobutanol reacts with a molecule of 1-butanol (**R7**).

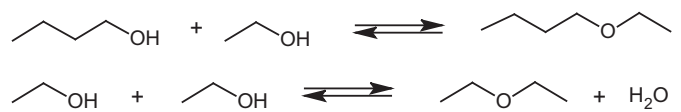


No significant change was observed in olefin concentration despite the addition of isobutanol to the reaction medium. Olefin 2-methyl propene (isobutylene) consequence of isobutanol intermolecular dehydration was not detected at these reaction conditions, probably due to the low isobutanol initial concentration and conversion extent. However, even though the amount of olefins, which are the most problematic byproduct, hardly changes by the isobutanol presence in the initial reaction mixture, it should be avoided as it increases the formation of branched ethers which present worse performance properties than the linear ether [8].

#### 3.4.2. Influence of ethanol and acetone

Two new byproducts were mainly detected when ethanol and acetone were added into the feed composition: the major one was ethyl butyl ether (EBE) which is formed by the dehydration reaction between a molecule of 1-butanol and a molecule of ethanol (R8); the other one, detected only in very low amounts, was di-ethyl ether (DEE) which is the product of ethanol intermolecular dehydration (R9).

As it can be seen in Fig. 11 selectivity to DNBE decreased whereas EBE formation increased when the initial amount of ethanol rises even at high 1-butanol:ethanol initial ratios. Similarly, in the dehydration reaction of 1-octanol/ethanol mixtures at 150 °C over acidic ion exchangers, ethers with lower molecular weight are preferentially formed [33]. Under the present experimental conditions the small amount of DEE detected is due to the high initial 1-butanol:ethanol ratios. DEE must be avoided as it cannot be blended directly into commercial diesel fuels.



Regarding acetone reactivity, its condensation/dehydration forming mesityl oxide (MSO) and water over Amberlyst 16 in the temperature range 100–120 °C has been quoted [34]. Still, under the current experimental conditions acetone hardly react and only very low amounts of 2-propanol were detected (always less than 0.04% chromatographic area/g of catalyst). 2-Propanol could be the product of the acetone hydrogenation catalyzed by component of stainless steel tubing's and reactor walls such as nickel or iron. The amount of olefins (1-butene, trans-2-butene and cis-2-butene) and the branched ether 1-(1-methylpropoxy)butane did not experiment significant changes despite ethanol/acetone addition. Comparing the catalytic behavior of the three resins it can be concluded that, as found when isobutanol was added, the presence of ethanol and acetone in the medium does not change significantly the general trend observed when 1-butanol is free of impurities.

## 4. Conclusions

Sulfonic S/DVB resins are shown to be suitable catalysts for the dehydration reaction of 1-butanol to di-n-butyl ether in the liquid phase. Activity (reaction rate and conversion of 1-butanol) is enhanced with higher acid capacity (oversulfonated resins) and with medium values of swollen polymer volume (0.823–1.245 cm<sup>3</sup>/g). Very high polymer concentration results in a very dense polymer mass, poorly accessible to 1-butanol. On the contrary, very low polymer concentration corresponds to a greatly expanded polymer which results in a large distance between its active centers. As a result, the probability of disposing the precise conformation of sulfonic groups to form the reaction intermediate lessens and 1-butanol conversion decreases. Amberlyst 36 (oversulfonated, medium values of %DVB) has proved to be the most active catalysts tested. However, gel-type resins (which have a

flexible morphology and are able to greatly swell in the reaction medium) and the resins Amberlyst-70 and Amberlyst-46 are more selective to DNBE; the resin Amberlyst 121 being the most selective. DNBE formation follows an *S<sub>N</sub>2* reaction mechanism in which 2 molecules of 1-butanol are involved, whereas dehydration to butenes occurs through a monomolecular reaction of elimination, E1. As a consequence, in highly expanded polymers the *S<sub>N</sub>2* reaction is not limited by steric hindrance yielding higher selectivity to the linear ether. In addition, a clear relationship between selectivity and H<sup>+</sup>/V<sub>sp</sub> ratio has been observed; the resins with lowest H<sup>+</sup>/V<sub>sp</sub> being the most selective.

The presence of 2-methyl-1-propanol in the initial reactant mixture enhances the formation of branched ethers, which have worse properties as diesel components than linear ones. However no significant changes were observed in the concentration of olefins which are the most troublesome byproducts regarding the sought properties for fuel additives. On the other hand, the presence of ethanol and acetone leads to the formation of ethyl butyl ether and di-ethyl ether but in a much lesser extent. Di-ethyl ether must be avoided as it cannot be blended directly into commercial diesel fuels.

## Acknowledgments

Financial support was provided by the Science and Education Ministry of Spain (project: CTQ2010-16047). The authors thank Rohm and Haas France and Purolite for providing Amberlyst and

CT ion-exchange resins, respectively. We also thank Dr. Karel Jerabek of Institute of Chemical process Fundamentals (Prague, Czech Republic) for the morphological analyses made by the ISEC method.

## References

- [1] L.S. Ott, B.L. Smith, T.J. Bruno, *Energy Fuels* 22 (2008) 2518–2526.
- [2] M.N. Nabi, D. Kannan, J.E. Hustad, M.M. Rahman, International Conference on Mechanical Engineering, Dhaka, Bangladesh, 2009.
- [3] A. Golubkov, Motor Fuels for Diesel Engines. Patent WO2001018154 A1 (2001).
- [4] T.J.A. Alander, A.P. Leskinen, T.M. Raunemaa, L. Rantanen, *Environ. Sci. Technol.* 38 (2004) 2707–2714.
- [5] A. Arteconi, A. Mazzarini, G. Di Nicola, *Water Air Soil Pollut.* 221 (2011) 405–423.
- [6] I. Sezer, A. Bilgin, *Energy Fuels* 22 (2008) 1341–1348.
- [7] R.L. McCormick, J.D. Ross, M.S. Graboski, *Environ. Sci. Technol.* 31 (4) (1997) 1144–1150.
- [8] G.C. Pecci, M.G. Clerici, F. Giavazzi, F. Ancillotti, M. Marchionna, R. Patrini, *IX Int. Symp. Alcohol Fuels* 1 (1991) 321–326.
- [9] M. Marchionna, R. Patrini, F. Giavazzi, G.C. Pecci, Symposium on Removal of Aromatics, Sulfur and Alkenes from Gasoline and Diesel, 212th National Meeting, ACS, 1996, pp. 585–589.
- [10] L.S. Starkey, Introduction to Strategies for Organic Synthesis, Wiley, Hoboken, NJ, 2012 (Chapter 3.3).
- [11] R.A. Sheldon, H. van Bekkum, Fine Chemical through Heterogeneous Catalysis, Wiley-VCH, Weinheim (Germany), 2001 (Chapter 6.5).
- [12] Chemsystems Perp Program, Oxo Alcohols PERP 06/07-08. [www.chemsystems.com](http://www.chemsystems.com) (07/2013).
- [13] T. Tsuchida, S. Sakuma, T. Takeguchi, W. Ueda, *Ind. Eng. Chem. Res.* 45 (2006) 8634–8642.
- [14] R. Cascone, *Chem. Eng. Progress* 104 (8) (2008) S4–S9.
- [15] <http://www.biofuelstp.eu/butanol.html> European Biofuels Technology Platform (07/2013).
- [16] Anonymous, *Chem. Eng. Progress* 103 (2007) 14.
- [17] R.J.J. Nel, A. de Clerk, *Ind. Eng. Chem. Res.* 48 (2009) 5230–5238.
- [18] M.A. Makarova, E.A. Paukshtis, J.M. Thomas, C. Williams, K.I. Zamaraev, *J. Catal.* 149 (1994) 36–51.
- [19] F.M. Bautista, B. Delmon, *Appl. Catal. A: General* 130 (1995) 47–65.
- [20] P. Brandão, A. Philippou, J. Rocha, M.W. Anderson, *Catal. Lett.* 80 (3–4) (2002) 99–102.

- [21] J.H. Choi, J.K. Kim, D.R. Park, S. Park, J. Yi, I.K. Song, *Catal. Commun.* 14 (2011) 48–51.
- [22] J.K. Kim, J.H. Choi, J.H. Song, J. Yi, I.K. Song, *Catal. Commun.* 27 (2012) 5–8.
- [23] J. Tejero, F. Cunill, M. Iborra, J.F. Izquierdo, C. Fit  , *J. Mol. Catal. A: Chem.* 182 (2002) 541–554.
- [24] R. Bringu  , M. Iborra, J. Tejero, J.F. Izquierdo, F. Cunill, C. Fit  , V.F. Cruz, *J. Catal.* 244 (2006) 33–42.
- [25] E. Medina, R. Bringu  , J. Tejero, M. Iborra, C. Fite, *Appl. Catal. A: General* 374 (2010) 41–47.
- [26] C. Casas, R. Bringu  , E. Ram  rez, M. Iborra, J. Tejero, *Appl. Catal. A: General* 396 (2011) 129–139.
- [27] K. Jerabek, L. Hantova, Z. Prokop, 12th International Congress on Catalysis, Granada (Spain), 2000.
- [28] S. Fisher, R. Kunnin, *Anal. Chem.* 27 (1955) 1191–1194.
- [29] A.G. Ogston, *Trans. Faraday Soc.* 54 (1958) 1754–1757.
- [30] G.A. Olah, T. Shamma, G.K. Surya Prakash, *Catal. Lett.* 46 (1997) 1–4.
- [31] K.P.C. Vollhardt, N.E. Schore, *Qu  mica Org  nica*, 2nd ed., Omega, Barcelona, Spain, 2000 (Chapter 9.3).
- [32] S. Kotsarenko, L.V. Malysheva, *Kinet. Katal.* 24 (1983) 877–882.
- [33] J. Guilera, R. Bringu  , E. Ram  rez, M. Iborra, J. Tejero, *Ind. Eng. Chem. Res.* 51 (2012) 16525–16530.
- [34] E. du Toit, R. Schwarzer, W. Nicol, *Chem. Eng. Sci.* 59 (2004) 5545–5550.